ELSEVIER

Journal of Molecular Catalysis B: Enzymatic 16 (2002) 283–291

JOURNAL OF MOLECULAR CATALYSIS B: ENZYMATIC

www.elsevier.com/locate/molcatb

Preparation and characterization of YADH-bound magnetic nanoparticles

Dong-Hwang Chen*, Min-Hung Liao

Department of Chemical Engineering, National Cheng Kung University, Tainan 701, Taiwan, ROC

Received 2 October 2001; received in revised form 1 November 2001; accepted 1 November 2001

Abstract

The covalently binding of yeast alcohol dehydrogenase (YADH) to magnetic nanoparticles via carbodiimide activation was studied. The magnetic nanoparticles Fe_3O_4 with a mean diameter of 10.6 nm were prepared by co-precipitating Fe^{2+} and Fe^{3+} ions in an ammonia solution and treating under hydrothermal conditions. Transmission electron microscopy (TEM) micrographs showed that the magnetic nanoparticles remained discrete and had no significant change in size after binding YADH. X-ray diffraction (XRD) patterns indicated both the magnetic nanoparticles before and after binding YADH were pure Fe_3O_4. Magnetic measurement revealed the resultant magnetic nanoparticles were superparamagnetic characteristics, and their saturation magnetization was reduced only slightly after enzyme binding. The analysis of Fourier transform infrared (FTIR) spectroscopy confirmed the binding of YADH to magnetic nanoparticles and suggested a possible binding mechanism. In addition, the measurement of protein content revealed that the maximum weight ratio of YADH bound to magnetic nanoparticles was 0.125, below which the binding efficiency of YADH was almost 100%. The kinetic measurements indicated the bound YADH retained 62% of its original activity and exhibited a 10-fold improved stability than did the free enzyme. The maximum specific activities and Michaelis constants were also determined.

Keywords: Yeast alcohol dehydrogenase; Magnetic nanoparticles; Bound

1. Introduction

Alcohol dehydrogenase which catalyzes the oxidation of alcohols and the reduction of carbonyl compounds such as aldehydes and ketones has attracted attention because of its potential applications in the production of various starting materials and intermediates in chemical industry, the synthesis of chiral compounds, the regeneration of coenzymes NAD(P) and NAD(P)H, and biosensors [1–3]. Unfortunately, its stability is poor and hence limits its practical applications [4,5].

Immobilization is one of the efficient methods to improve enzyme stability. Many organic and inorganic substances have been used as the support materials. Among them, magnetic particles receive considerable attention because of their wide uses in the immobilization of proteins and enzymes [6–10], bioseparation [11–14], immunoassays [15,16], drug delivery [15,17,18], biosensors [19], protein assay [20] and so on. Their sizes are usually in the submicrometer to micrometer. In the recent years, the nanosized magnetic particles receive increasing attention with the rapid development of nanostructured materials and nanotechnology in the fields of biotechnology and medicine [21,22]. Using magnetic nanoparticles as the support of immobilized enzymes has the following advantages: (1) higher specific surface area

* Corresponding author. Tel.: +886-6-2757575x62680; fax: +886-6-2344496.
E-mail address: chendh@mail.ncku.edu.tw (D.-H. Chen).

1381-1177/02/$ – see front matter
PII: S1381-1177(01)00074-1

was obtained for the binding of a larger amount of enzymes, (2) lower mass transfer resistance and less fouling, and (3) the immobilized enzymes can be selectively separated from a reaction mixture by the application of a magnetic field [6].

Magnetite (Fe_3O_4) is one of the famous magnetic materials in common use. Due to strong magnetic property and low toxicity, its applications in biotechnology and medicine has gained significant attention [23]. Many bioactive substances such as enzymes, proteins, antibodies, and anticancer agents have been bound to it [6–20]. The binding is commonly accomplished through the surface coating with polymers, the use of coupling agents or crosslinking reagents, and encapsulation. Recently, a new method for the direct binding of proteins such as bovine serum albumin via carbodiimide activation was reported [24,25]. This method is notable due to its simplicity and high efficiency.

The immobilization of alcohol dehydrogenase on various supports has been investigated by several researchers [4,26–28]. However, its immobilization on magnetite nanoparticles was reported only by Shinkai et al. [29], and the residual activity was relatively low (12%). In this work, the direct binding of YADH to magnetite nanoparticles via carbodiimide activation was investigated. The size, structure, and magnetic property of the resultant nanoparticles were characterized by transmission electron microscopy (TEM), X-ray diffraction (XRD), and the superconducting quantum interference device (SQUID) magnetometer. The binding of YADH to magnetic nanoparticles was confirmed by Fourier transform infrared (FTIR) spectroscopy. The stability and activity of bound YADH were also examined.

2. Materials and methods

2.1. Chemicals

Crystallized and lyophilized alcohol dehydrogenase (EC1.1.1.1) from baker's yeast (No. A-3263), β-nicotinamide adenine dinucleotide, reduced form (NADH, N-8129), and carbodiimide were purchased from Sigma (St. Louis, MO). Bio-Rad reagent for protein assay was obtained from Bio-Rad Lab. (Hercules). Ferric chlorides, 6-hydrate and ferrous chloride tetrahydrate were the products of J.T. Baker (Phillipsburg) and Fluka (Buchs), respectively. 2-Butanone was an analytic grade reagent of Ferak (Germany). Ammonium hydroxide (29.6%) was supplied by TEDIA (Fairfield). Tris(hydroxymethyl)aminomethane (Tris) and hydrochloric acid were the guaranteed reagents of E. Merck (Darmstadt). The water used throughout this work was the reagent-grade water produced by Milli-Q SP ultra-pure-water purification system of Nihon Millipore Ltd., Tokyo. All other chemicals were the guaranteed or analytic grade reagents commercially available and used without further purification.

2.2. Preparation of magnetic nanoparticles

Magnetic nanoparticles Fe_3O_4 were prepared by co-precipitating Fe^{2+} and Fe^{3+} ions by ammonia solution and treating under hydrothermal conditions [24,25]. The ferric and ferrous chlorides (molar ratio 2:1) were dissolved in water at a concentration of 0.3 M iron ions. Chemical precipitation was achieved at 25 °C under vigorous stirring by adding NH_4OH solution (29.6%). During the reaction process, the pH was maintained at about 10. The precipitates were heated at 80 °C for 30 min, then washed several times with water and ethanol, and finally dried in a vacuum oven at 70 °C.

2.3. Binding of YADH to magnetic nanoparticles

For the binding of YADH, 20–100 mg of magnetic nanoparticles were first added to 2 ml of buffer A (0.003 M phosphate, pH 6, 0.1 M NaCl). Then, the reaction mixture was sonicated for 10 min after adding 0.5 ml of carbodiimide solution (0.025 g/ml in buffer A). Finally, 2.5 ml of YADH solution (0.8–2.4 mg/ml in buffer A) was added and the reaction mixture was sonicated for 30 min. The preliminary experiment showed the residual activity of bound YADH obtained at 4 °C (62%) was much higher than that obtained at 25 °C (17%). So, in this work, the binding process was carried out at a constant temperature of 4 °C. The YADH-bound magnetic nanoparticles were recovered from the reaction mixture by placing the bottle on a permanent magnet with a surface magnetization of 3000 G. The magnetic particles settled within 1–2 min. The supernatant was used for the protein analysis. The precipitates were washed with buffer A,

then buffer B (0.1 M Tris, pH 8.0, 0.1 M NaCl), and then directly used for the measurements of activity and stability. It deserves to be mentioned that NaCl was used for the flocculation of magnetic nanoparticles [9]. Its addition could accelerate the magnetic separation, particularly in alkaline solutions.

2.4. Characterization

The size and morphology of magnetic nanoparticles were observed by TEM using a JEOL model JEM-1200EX at 80 kV. The sample for TEM analysis was obtained by placing a drop of the magnetic nanoparticles-dispersed ethanol solution onto a Formvar covered copper grid and evaporated in air at room temperature. Before withdrawing the sample, the dispersed solution was sonicated for 1 min to obtain the better particle dispersion on the copper grid. For each sample, over 120 particles from different parts of the grid were used to estimate the mean diameter and size distribution of particles. XRD measurement was performed on a Rigaku D/max III V X-ray diffractometer using Cu Kα radiation ($\lambda = 0.1542$ nm). The magnetic measurement was done using a SQUID magnetometer (MPMS7, quantum design). The amount of bound YADH was determined by measuring the unbound protein content in the supernatant after binding process by the colorimetric method at 595 nm using the Bio-Rad reagent for protein assay with bovine serum albumin as the standard. The binding of YADH to the magnetic nanoparticles was checked using FTIR. All the YADH-bound magnetic nanoparticles used for the analyses of TEM, XRD, SQUID, and FTIR in this work had a binding of 5 mg YADH on 100 mg Fe_3O_4.

2.5. Activity measurement

The activity of bound YADH was determined by measuring the initial reduction rate of 2-butanone by YADH at the desired temperature following the decrease of NADH concentration at 340 nm on a Hitachi U-3000 spectrophotometer. Generally, 2 ml of NADH solution (0.5 mM in buffer B) was added to the test tube containing 100 mg of YADH-bound magnetic nanoparticles. After mixing by vortex, 3 ml of 2-butanone solution (0.1 M in buffer B) was added. After mixing for several minutes by vortex, the liquid solution separated from the magnetic nanoparticles via a permanent magnet was used for the analysis of NADH concentration. Unless otherwise stated, the amount of bound YADH to 100 mg magnetic nanoparticles was 5 mg YADH. The activity of YADH was determined in buffer B at 25 °C, and the concentrations of NADH, 2-butanone, YADH in the reaction mixture were 0.2 mM, 0.06 M, and 1.0 mg/ml, respectively.

For free YADH, the activity measurement was done following the similar procedures and conditions for the bound YADH except that free YADH was used and magnetic separation was unnecessary.

2.6. Stability measurement

The storage stabilities of bound and free YADH were examined by assaying their residual activities at 25 °C after being incubated in buffer B at 4 or 25 °C for a required period. The thermal stabilities of bound and free YADH were investigated by measuring their residual activities at 25 °C after being incubated in buffer B for 30 min at the desired temperatures.

2.7. Reusability assay

The reusability of bound YADH was examined by conducting the activity measurement of bound YADH at 25 °C at time intervals of 10 min. After each activity measurement, the bound YADH was separated magnetically and washed several times with buffer B under sonication. Then, the fresh NADH and 2-butanone solutions were added to the bound YADH in sequence and the next activity measurement was carried out.

2.8. Determination of kinetic parameters

The kinetic parameters of free and immobilized YADH were determined by measuring their activity in buffer B at 25 °C. The concentrations of NADH, 2-butanone, YADH in the reaction mixture were 0.10–0.25 mM, 0.06–0.15 M, and 1.0 mg/ml, respectively.

3. Results and discussion

3.1. Binding efficiency

By assaying the unbound protein in the supernatant after binding process, it was found that, with

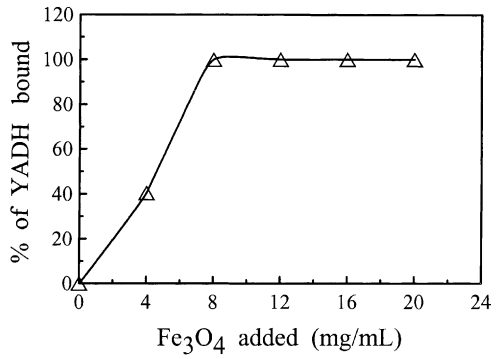

Fig. 1. Effect of the amount of Fe_3O_4 nanoparticles added on the percentage of bound YADH. [YADH] = 1 mg/ml.

increasing the amount of Fe_3O_4 added at a constant YADH amount of 1 mg/ml, the percentage of bound YADH increased and then remained at 100% when the amount of Fe_3O_4 added was above 8 mg/ml as indicated in Fig. 1. Accordingly, the maximum weight ratio of bound YADH to Fe_3O_4 nanoparticles could be determined to be 0.125. When the weight ratio of YADH to Fe_3O_4 was below 0.125, YADH could be completely bound to Fe_3O_4 nanoparticles. In addition, the density of Fe_3O_4 is 5.18 g/cm^3 and the molecular weight of YADH was about 141,000 [30]. Assuming the resultant Fe_3O_4 nanoparticles were spherical, it could be estimated that averagely one YADH molecule was bound to a Fe_3O_4 particle when the weight ratio of YADH to Fe_3O_4 was about 0.086. Thus, the binding of YADH to Fe_3O_4 nanoparticles in this work has been achieved at a level of monomolecular binding.

3.2. Particle size and structure

The typical TEM micrographs and the size distribution for the magnetic nanoparticles without and with bound YADH are shown in Fig. 2. It was clear that the naked Fe_3O_4 particles were essentially very fine and monodisperse with a mean diameter of 10.6 ± 2.6 nm. After binding YADH, the particles remained discrete and had a mean diameter of 11.3 ± 3.3 nm, similar to that of unbound ones. This reveals that the binding process did not significantly result in the agglomeration and the change in size of particles. This could be attributed to the reaction occurred only on the particle surface and, as stated above, a particle bound only one YADH molecule.

Fig. 3 shows the XRD patterns for the magnetic nanoparticles without and with bound YADH. Six characteristic peaks for Fe_3O_4 ($2\theta = 30.1$, 35.5, 43.1, 53.4, 57.0 and 62.6°), marked by their indices ((220), (311), (400), (422), (511), and (440)), were observed for both samples. This revealed that the resultant particles were pure Fe_3O_4 with a spinel structure. Also, the binding process did not result in the phase change of Fe_3O_4.

3.3. Magnetic property

The plots of magnetization versus magnetic field (M–H loop) at 25 °C for the typical magnetic nanoparticles without and with bound YADH are illustrated in Fig. 4. The very weak hysteresis revealed the resultant magnetic nanoparticles were nearly superparamagnetic. This could be attributed to the fact that the magnetic nanoparticles were so small that they may be considered to have a single magnetic domain. From the plots of M versus H and their enlargements near the origin as shown in the insets in Fig. 4, the saturation magnetization (M_s), remanent magnetization (M_r), coercivity (H_c), and squareness ($S_r = M_r/M_s$) could be determined to be 63.3 emu/g, 1.13 emu/g, 9.2 Oe, and 0.018, respectively, for naked magnetic nanoparticles, and 61.0 emu/g, 0.85 emu/g, 6.8 Oe, and 0.014, respectively, for YADH-bound magnetic nanoparticles.

The saturation magnetization of Fe_3O_4 nanoparticles was reduced to 69% of the bulk Fe_3O_4 (92 emu/g) [31]. The reduction in M_s might be due to the decrease in particle size and the accompanied increase in surface area. It is known that the energy of a magnetic particle in an external field is proportional to its size via the number of magnetic molecules in a single magnetic domain. When this energy becomes comparable to thermal energy, thermal fluctuations will significantly reduce the total magnetic moment at a given field [32,33]. It is also known that the magnetic molecules on the surface lack complete coordination and the spins are likewise disordered [32–35]. So, the large surface-to-volume ratio for nanoparticles may be another factor that leads to the decrease in M_s. In addition, the disorderd structure in amorphous materials and at the interface such as that found at a grain boundary has been shown to cause a decrease in the effective magnetic moment [36]. Therefore, another possible reason for the diminution in M_s might be

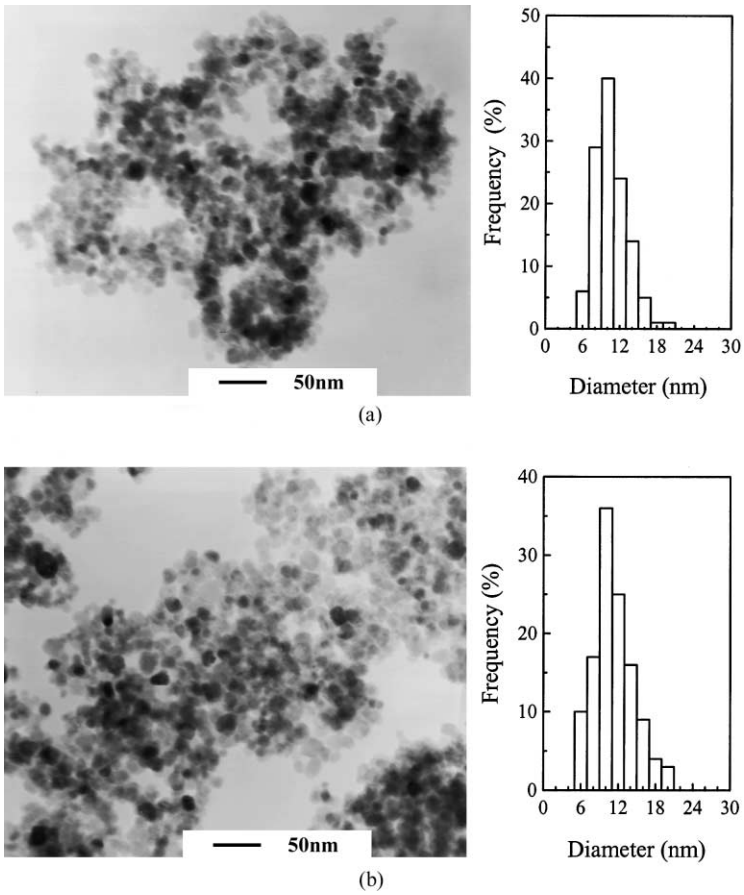

Fig. 2. Transmission electron micrographs and size distributions of magnetic nanoparticles without (a), and with (b) bound YADH. YADH/Fe_3O_4= 1/20 (w/w).

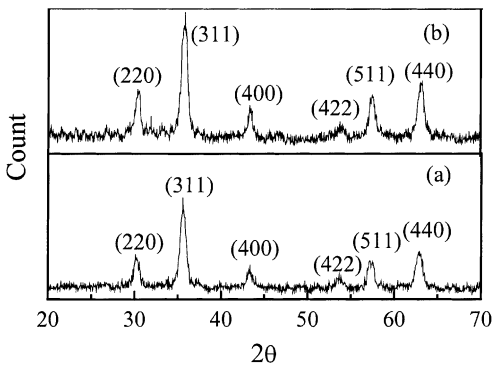

Fig. 3. XRD patterns of magnetic nanoparticles without (a), and with (b) bound YADH. YADH/Fe_3O_4= 1/20 (w/w).

the incomplete crystallization of Fe_3O_4 nanoparticles, which led to amorphous impurities undetectable by XRD. Finally, the electron exchange between ligand and surface atoms could also quench the magnetic moment [37]. Although the magnetic nanoparticles have been washed before the magnetic measurement, the investigation on FTIR spectra (shown later) indicated the $–NH_2$ ligand might be present on the surface of Fe_3O_4 nanoparticles. This might be another reason causing the decrease in M_s value.

The M_s value for YADH-bound magnetic nanoparticles was lower slightly than that for the naked ones. This might be resulted from the binding of YADH on the particle surface, which might quench the magnetic moment. In addition, the reduction in M_s value due to enzyme binding was only 3.6%. This might be due

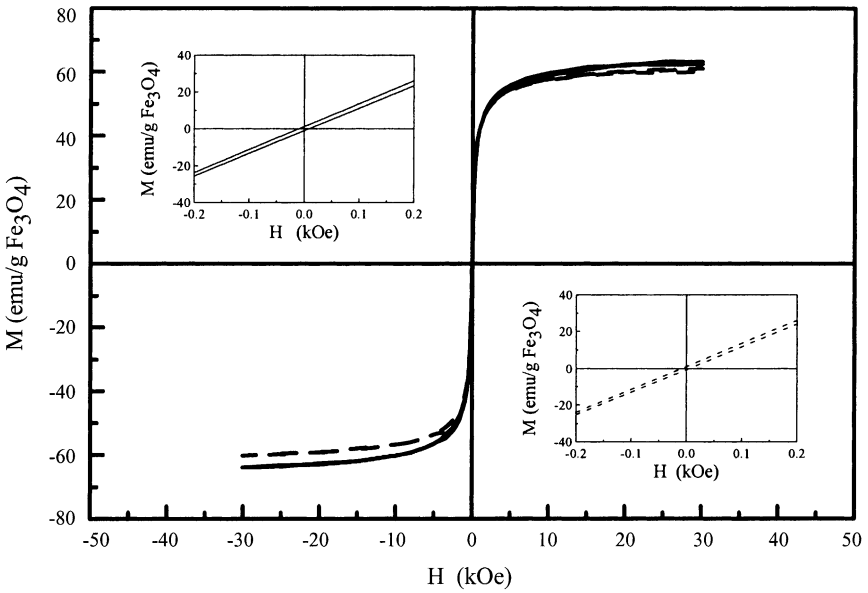

Fig. 4. Magnetization vs. magnetic field for the magnetic nanoparticles without (——) and with (- - -) bound YADH at 25 °C. YADH/Fe_3O_4= 1/20 (w/w).

to the fact that about only one YADH molecule was bound to a Fe_3O_4 nanoparticle in this work.

The M_r, H_c, and S_r values were so small that they were the superparamagnetic characteristics and implied that the thermal energy to demagnetize became dominant over spontaneous magnetization. After binding YADH, these values all were reduced. This might also be resulted from the enzyme binding. However, because these values were so small that the differences between them and those for naked magnetic nanoparticles were within the deviations, further discussion seems unnecessary.

3.4. Mechanism of binding

The binding of YADH to magnetic nanoparticles was confirmed by FTIR analysis. Fig. 5 shows the FTIR spectra for the solid state pure YADH, naked Fe_3O_4, and YADH-bound Fe_3O_4. It was obvious that the characteristic bands of protein (i.e. YADH) at 1648 and 1540 cm^{-1} were present in pure YADH and in the YADH-bound Fe_3O_4 nanoparticles, confirming the binding of YADH to Fe_3O_4 nanoparticles. The weak characteristic bands of proteins for the YADH-bound Fe_3O_4 should be owing to the low enzyme loading.

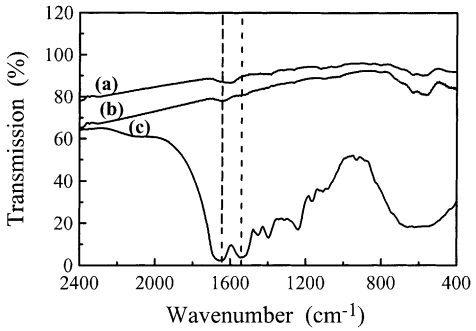

Fig. 5. FTIR spectra of the magnetic nanoparticles without (a), with (b) bound YADH, and the pure YADH (c). YADH/Fe_3O_4= 1/20 (w/w).

In addition, it is noted that a characteristic band of $–NH_2$ at 1625 cm^{-1} was observed in naked Fe_3O_4 nanoparticles. After binding YADH, this characteristic band disappeared. Thus, it was suggested that the binding was accomplished via the reaction between the amine group on Fe_3O_4 nanoparticles and the carboxyl group of YADH after being activated by carbodiimide. As for the amine group, it might be formed due to the use of concentrated ammonia solution during the co-precipitation of Fe^{2+} and Fe^{3+} ions.

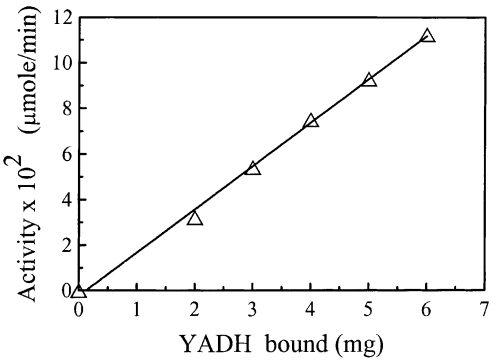

Fig. 6. Effect of the amount of bound YADH on its activity at 25 °C. Fe_3O_4; 100 mg in 5 ml solution.

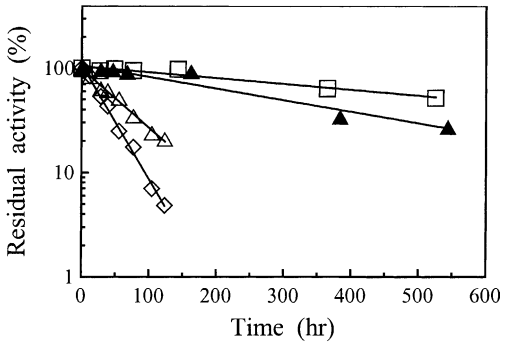

Fig. 7. Storage stabilities of the bound YADH at 4 °C (□) and 25 °C (▲)and the free YADH at 4 °C (△) and 25 °C (◇).

3.5. Activity

Fig. 6 indicates the activities of different amount of YADH (0–6 mg) bound on 100 mg Fe_3O_4 nanoparticles. Under this condition, YADH was completely bound according to the investigation on binding efficiency. The linear relationship revealed that the specific activity of bound YADH to Fe_3O_4 nanoparticles remained constant (0.0197 μmol/(min mg)). In the concentration range, the specific activity of free YADH was determined to be 0.0319 μmol/(min mg). The residual activity was 62%, much higher than that obtained using other method for alcohol dehydrogenase as reported by Shinkai et al. (12%) [29]. Thus, this immobilization method allowed not only the complete binding of YADH but also the relatively high activity retention.

3.6. Stability

Fig. 7 shows that the storage stabilities of bound and free YADH at 4 and 25 °C in a semi-log plot. After an incubation time of 120 h, the residual activities of free YADH at 4 and 25 °C were 20 and 4.5%. However, the bound YADH retained 60 and 30% activity at 4 and 25 °C, respectively, over a period of 500 h. This revealed that the storage stability of YADH was improved significantly after being bound to Fe_3O_4 nanoparticles. In addition, the linear relationship revealed that both the deactivation of bound and free YADH followed the first-order rate equation. The corresponding first-order deactivation rate constants for free YADH were 0.013 and 0.0252 h^{-1} at 4 and 25 °C, respectively; while those for bound YADH were 0.0013 and 0.0026 h^{-1}, respectively. After immobilization, the first-order deactivation rate constants of YADH were reduced to 10% of their original values at both temperatures.

The thermal stabilities of free and bound YADH after an incubation period of 30 min in the temperature range of 25 to 65 °C were indicated in Fig. 8. For free YADH, almost no activity was retained when incubation temperature was above 55 °C. However, the activity of bound YADH was not significantly reduced when incubation temperature was below 55 °C. Even at an incubation temperature of 65 °C, the bound YADH still had a residual activity of 90%. This revealed clearly that the thermal stability of YADH was improved largely after being bound to Fe_3O_4 nanoparticles.

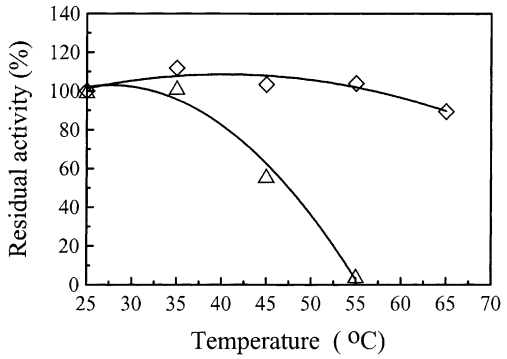

Fig. 8. Thermal stabilities of the bound (◇) and the free (△) YADH.

According to the above, the immobilization method used in this work was quite efficient for the improvement of YADH stability.

3.7. Reusability

Reusability of immobilized enzymes is important for their practical application. According to our investigation, the activity of bound YADH had no significant loss after being reused 13 times within 2 h. This indicated the resultant YADH-bound magnetic nanoparticles had excellent reusability.

3.8. Kinetic parameters

Alcohol dehydrogenase has been known to operate usually by a random-order equilibrium mechanism or a compulsory-order mechanism, with one ternary complex. Since the plots of $1/V$ against 1/[2-butanone] at a series of NADH concentrations (0.10–0.25 mM) for both the free and immobilized YADH at 25 °C were found to be a series of parallel lines and the plots of the intercepts of these parallel lines against 1/[NADH] also yielded straight lines. The rate equation for the reduction of 2-butanone (0.06–0.15 M) by YADH could be expressed as [38]

$$V = \frac{V_{\max}}{1 + K_{\mathrm{m}}^{\mathrm{A}}/[\mathrm{NADH}] + K_{\mathrm{m}}^{\mathrm{B}}/[\text{2-butanone}]}$$

where V and $V_{\max}$ are the specific activity and maximum specific activity, respectively; and $K_{\mathrm{m}}^{\mathrm{A}}$ and $K_{\mathrm{m}}^{\mathrm{B}}$ are the Michaelis constants for NADH and 2-butanone, respectively. The kinetic parameters for free and immobilized YADH were determined as listed in Table 1. The decrease in $V_{\max}$ value might be due to the denaturation of enzyme during the immobilization process. The increase in $K_{\mathrm{m}}^{\mathrm{A}}$ and $K_{\mathrm{m}}^{\mathrm{B}}$ values after immobilization revealed that the immobilized YADH had a lower affinity to NADH and 2-butanone. This might be due to the fixation of YADH molecules and/or the change in the property of active sites for the binding of NADH and 2-butanone after enzyme immobilization.

Table 1
The kintetic parameters for free and immobilized YADH

YADH	$K_{\mathrm{m}}^{\mathrm{A}}$ (mM)	$K_{\mathrm{m}}^{\mathrm{B}}$ (mM)	$V_{\max}$ (μmol/(min mg))
Free	0.48	0.36	0.27
Immobilized	0.62	0.43	0.23

4. Conclusions

Magnetic nanoparticles Fe_3O_4 were prepared and YADH was directly bound to them via carbodiimide activation. The analyses of TEM and XRD indicated the resultant magnetic nanoparticle were pure Fe_3O_4 with a mean diameter of 10.6 nm, and the binding process did not cause the changes in particle size and structure. The magnetic measurement showed the resultant Fe_3O_4 nanoparticles were superparamagnetic and the binding of YADH only slightly reduced their saturation magnetization. From FTIR spectra, the binding of YADH to Fe_3O_4 was confirmed and the corresponding mechanism could be suggested. The binding of YADH to Fe_3O_4 nanoparticles was achieved at a level of monomolecular binding. The maximum weight ratio of bound YADH to Fe_3O_4 nanoparticles was about 0.125, below which the binding efficiency of YADH was 100%. After being bound, YADH had a residual activity of 62%, good reusability, and significantly better storage and thermal stabilities than did the free enzyme. The kinetic parameters, including maximum specific activities and Michaelis constants, were determined and revealed the affinity of YADH to NADH and 2-butanone decreased after immobilization. This work will be helpful for the practical application of YADH.

Acknowledgements

This work was performed under the auspices of the National Science Council of the Republic of China, to which the authors wish to express their thanks.

References

[1] W. Hummel, M.R. Kula, Eur. J. Biochem. 184 (1989) 1–13.
[2] J.B. Jones, Tetrahedron 42 (1986) 3351–3403.
[3] A.K. Williams, J.T. Hupp, J. Am. Chem. Soc. 120 (1998) 4366–4371.
[4] H. Ooshima, Y. Genko, Y. Harano, Biotechnol. Bioeng. 23 (1981) 2851–2862.
[5] B. Orlich, H. Berger, M. Lade, R. Schomäcker, Biotechnol. Bioeng. 70 (2000) 638–646.

[6] P.J. Halling, P. Dunnill, Enzyme Microb. Technol. 2 (1980) 2–10.
[7] M.Y. Arica, H. Yavuz, S. Patir, A. Denizli, J. Mol. Catal. B Enzymatic 11 (2000) 127–138.
[8] H. Kobayashi, T. Matsunaga, J. Colloid Interface Sci. 141 (1991) 505–511.
[9] A. Kondo, H. Fukuda, J. Ferment. Bioeng. 84 (1997) 337–341.
[10] M. Reetz, A. Zonta, V. Vijayakrishnan, K. Schimossek, J. Mol. Catal. A Chem. 134 (1998) 251–258.
[11] S. Roath, J. Magn. Magn. Mater. 122 (1993) 329–334.
[12] S.V. Sonti, A. Bose, J. Colloid Interface Sci. 170 (1995) 575–585.
[13] X.D. Tong, B. Xue, Y. Sun, Biotechnol. Prog. 17 (2001) 134–139.
[14] T.M. Cocker, C.J. Fee, R.A. Evans, Biotechnol. Bioeng. 53 (1997) 79–87.
[15] W. Schütt, C. Grüttner, U. Häfeli, M. Zborowski, J. Teller, H. Putzar, C. Schümichen, Hybridoma 16 (1997) 109–117.
[16] F. Sauzedde, A. Elaissari, C. Pichot, Macromol. Symp. 151 (2000) 617–623.
[17] W. Schütt, C. Grüttner, J. Teller, F. Westphal, U. Häfeli, B. Paulke, P. Goetz, W. Finck, Artif. Organs 23 (1999) 98–103.
[18] S.R. Rudge, T.L. Kurtz, C.R. Vessely, L.G. Catterall, D.L. Williamson, Biomaterials 21 (2000) 1411–1420.
[19] A.R. Varlan, J. Suls, P. Jacobs, W. Sansen, Biosens. Bioelectron. 10 (1995) 15–19.
[20] T.N. Krogh, T. Berg, P. Højrup, Anal. Biochem. 274 (1999) 153–162.
[21] J.L. West, N.J. Halas, Curr. Opin. Biotechnol. 11 (2000) 215–217.
[22] A. Curtis, C. Wilkinson, TIBTECH 19 (2001) 97–101.
[23] P.A. Dresco, V.S. Zaitsev, R.J. Gambino, B. Chu, Langmuir 15 (1999) 1945–1951.
[24] R.V. Mehta, R.V. Upadhyay, S.W. Charles, C.N. Ramchand, Biotechnol. Tech. 11 (1997) 493–496.
[25] M. Koneracká, P. Kopcanský, M. Antalík, M. Timko, C.N. Ramchand, D. Lobo, R.V. Mehta, R.V. Upadhyay, J. Magn. Magn. Mater. 201 (1999) 427–430.
[26] W. Schöpp, M. Grunow, Appl. Microb. Biotechnol. 24 (1986) 271–276.
[27] V. Bille, D. Plainchamp, S. Lavielle, G. Chassaing, J. Remacle, Eur. J. Biochem. 180 (1989) 41–47.
[28] F.C. Cochrane, H.H. Petach, W. Henderson, Enzyme Microb. Technol. 18 (1996) 373–378.
[29] M. Shinkai, H. Honda, T. Kobayashi, Biocatalysis 5 (1991) 61–69.
[30] M. Buhner, H. Sund, Eur. J. Biochem. 11 (1969) 73–79.
[31] V. Zaitsev, D.S. Filimonov, I.A. Presnyakov, R.J. Gambino, B. Chu, J. Colloid Interface Sci. 212 (1999) 49–57.
[32] K.V.P.M. Shafi, A. Gedanken, R. Prozorov, J. Balogh, Chem. Mater. 10 (1998) 3445–3450.
[33] D.H. Chen, S.H. Wu, Chem. Mater. 12 (2000) 1354–1360.
[34] S. Kurisu, T. Ido, H. Yokoyama, IEEE Trans. Magn. 23 (1987) 3137–3139.
[35] X. Batlle, X. Obradors, M. Medarde, J.R. Carvajal, M. Pernet, M.V. Regi, J. Magn. Magn. Mater. 124 (1993) 228–238.
[36] J.H. Hwang, V.P. Dravid, M.H. Teng, J.J. Host, B.R. Elliott, D.L. Johnson, T.O. Mason, J. Mater. Res. 12 (1997) 1076–1082.
[37] D.A. Vanleeuwen, J.M. Vanruitenbeek, L.J. Dejongh, A. Ceriotti, G. Pacchioni, O.D. Häberlen, N. Rösch, Phys. Rev. Lett. 73 (1994) 1432–1435.
[38] D.H. Chen, H.H. Chen, T.C. Huang, J. Chem. Tech. Biotechnol. 64 (1995) 217–224.